Report from UWEngineers

Qinghua Shen†, Wei Zhang†, Edrick Wong*, Brady Kieffer*, Xuemin (Sherman) Shen†
†Department of Electrical and Computer Engineering, University of Waterloo, Canada
*Department of System Engineering, University of Waterloo, Canada
Email: {q2shen, w99zhang, e55wong, bwkieffer, sshen}@uwaterloo.ca

***Abstract*—Electrical network frequency (ENF) has been used as evidence for location forensic. To determine location, we need accurate ENF information from noisy media files, select features of the ENF signal and the classify it based on previous knowledge of different grids.**

In this report, we first utilize multiple harmonics in frequency domain and an error correction method for accurate ENF estimation. Utilizing multiple harmonics faces the challenges of obtaining accurate signal to noise power ratio for weighted combine, we propose to use signal level to noise level as weights. Moreover, we exploit the fact that the ENF signal doesn't jump back and forth within a short period to design an error correction method, which is capable to get rid of inaccurate ENF estimation.

Second, we propose to combine the features both in time domain and frequency for grid classification. Based on the power signal characteristics, we propose to use crest factor and the ratio of first harmonic to the third harmonic to evaluate the distortion of power waveform. Moreover, we propose to categorize the signals based on nominal frequency and source type, and design proper features for each category via cross validation method. Our proposed classification scheme can achieve an accuracy rate of 94% for practice dataset.

Third, we design and build a small yet effective sensing circuit with accurate timing. We record 10 hours of data from both home, university in different time. Using our proposed classifier, we learnt that with confidence level of 47.6%, the waterloo grid is part of grid C. Since the confidence level is low, we consider waterloo grid belongs to "None of Above Options".

Below is our estimation for practice dataset with accuracy 94% AHCFF,BGIND,AFBDI,INCAE,FBBAD, CGNGB,DDCHG,EAIHI,EHECF,FCGEI.

Below is our estimation for test dataset with average confidence level of 79.35%. NDDCD,NNDAF,ACGBG,BFCEH,GHNNG, NFDAI,DNFNN,IECBD,ENIBE,FGCAG, CINIG,HAEFC,CNFDG,CEIGI,EICEC, BNBNA,DIFNG,AABIH,CCDBA,GBFBB

I. Introduction

Electrical network frequency (ENF) [2] has been exploited to be used for location forensic. Two facts make this idea promising. First, the ENFs for the regions with connected grid are the same. Second, ENF can be captured in sound and video recording. Thus, through extracting the ENF signal in a ransom request call, it is possible to identify the caller's location.

However promising, the wide adoption of ENF based location forensic faces challenges, without proper addressing, the performance of such a system may not be accepted. First, sound and video files contain significant noise for ENF extraction, making obtaining accurate ENF difficult. Second, many regions have similar ENF characteristics, making the classification based on ENF challenging.

In this project, we utilize multiple harmonics and propose to use error correction scheme to improve the accuracy of ENF estimation. Further, we propose to combine features in both time domain and frequency domain to increase the distance of different grids in feature space. Moreover, we propose to categorize the signals before classification to improve both efficiency and accuracy.

The reminder of this report is organized as follows. Section II explains our approach in obtaining accurate ENF via utilizing multiple harmonics and error correction. Section III dives into the details of feature selection and classification scheme. Section IV explains the design of the sensing circuits and show the ENF info for waterloo, ON. Section V summarizes this report and draws conclusions.

II. Extraction of ENF signals

In this section, we propose to use weighted multiple harmonics in frequency domain to improve accuracy in estimating frequency information. Since the exact signal power and noise power are unknown, we propose to use signal level to noise level as weights to combine multiple harmonics. Moreover, we exploit the fact that the ENF doesn't change back and forth within 15s to build an error correction scheme.

A. Multiple Harmonics Extraction

Extraction of multiple harmonics takes the following steps:

- Extract a segment of signal in time domain with fixed duration T_s;
- Perform Discrete Fourier Transform (DFT) with N_s point;
- Select the range of interests around kth ($k = 1, 2, ..., k_{max}$) harmonics. The range of the kth harmonic is $[k \cdot (f_{base} - f_r), k \cdot (f_{base} + k \cdot f_r)]$.

Here, we perform the extraction procedures for segments of fixed duration. The reason is that, to collect statistic information of the ENF, the samples need to be homogeneous. Thus, we obtain the ENF samples using fixed duration.

1) The choice of T_s : The duration T_s impacts the quality of ENF. For one hand, the duration T_s determines the frequency resolution. For DFT without zero padding, the frequency resolution is determined by $\frac{1}{T_s}$. Thus, longer T_s is preferred to improve frequency resolution. On the other hand, the duration T_s determines the amount of independent segments can be obtained from the original recorded signal. Let T_l denote the total length of the recorded signal, the amount of independent segments is $\frac{T_l}{T_s}$. Thus, the larger the fixed duration T_s, the

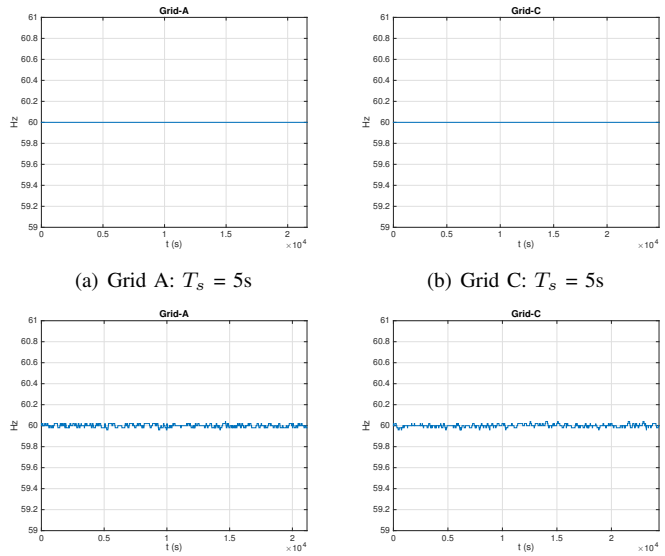

(a) Grid A: T_s = 5s (b) Grid C: T_s = 5s

(c) Grid A: T_s = 50s (d) Grid C: T_s = 50s

Fig. 1: Impact of Frequency Resolution for DFT without Zero Padding

smaller amount of independent segments. To obtain sufficient number of independent samples for calculating statistical information, the fixed segment duration T_s should not be too large. Considering above impacts, we set the fixed segment duration to be 5s, namely $T_s = 5s$.

2) Zero-Padding for Higher Frequency Resolution: What is the required frequency resolution? Since some grids are very stable and have small variation in ENF, low frequency resolution can make the variations in ENF unnoticeable. Fig. 1 shows the ENF signal of grid A and grid C under different fixed duration time T_s, where Fig. 2(a) and Fig. 2(b) with $T_s = 5s$ and Fig. 1(c) and Fig. 1(d) with $T_s = 50s$. We can observe that, given low frequency resolution such as $1./T_s = 0.2Hz$, grid A and grid C have the same ENF signal, thus are unable to distinguish. When resolution improves, the variation on each grid can be seen in Fig. 1(c) and Fig. 1(d).

In this report, we first exploit zero padding for resolution improvement. In order to reserve the frequency information without zero padding, we set the zero padding length to be $z_k FsT_s$, where z_k is an integer number. In this way, the frequency resolution is improved by z_k times [3].

B. Weighted Combination

Combining multiple harmonics has been proposed to improve the accuracy and robustness of frequency estimation [3]. The idea is what .... One of the major difficulty in combining is to determine weights for combining. [2] proposed to use average signal power to noise power as weights for harmonics combining. Specially, [2] consider the power spectrum in a range $[f_{base} - f_s, f_{base} + f_s]$ belongs to signal, whereas $[f_{base} - f_r, f_{base} - f_s) \cup (f_{base} - f_s, f_{base} - f_r]$ belongs to noise. There is an issue with this approach in practice. It may be difficult to determine the signal power range f_s, especially for the grid with large variations, such as grid B. If f_s is chosen too small, the actual signal power can be missed. On the other hand, if f_s is chosen too big, most noise will be considered as signal, which eventually makes the weights calculation less accurate.

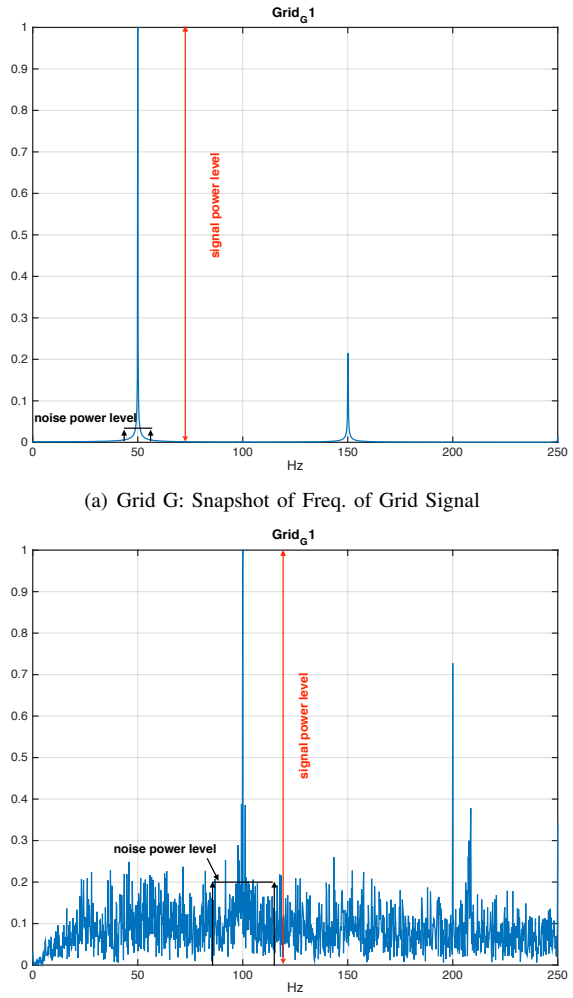

(a) Grid G: Snapshot of Freq. of Grid Signal

(b) Grid G: Snapshot of Freq. of sound Signal

Fig. 2: Illustration of Signal Power Level to Noise Power Level

To address the problem of unknown signal power range, we propose to use signal power level to noise power level as weights. The signal power level is the maximum PSD in the $[kf_{base} - kf_r, kf_{base} + kf_r]$ for the kth harmonics, and the noise power level is the average of the PSD in the $[kf_{base} - kf_r, kf_{base} + kf_r]$ for the kth harmonics, excluding the PSD of the signal. Fig. 2 shows examples of signal power level and noise power level. This approach reduces the risk of including too much noise power in signal power estimation. Using this approach, part of signal power is calculated as noise power, for signal power could be spread in frequency domain. Yet, it is also reasonable, for bigger spread of signal power in frequency domain means higher jitter, slewing or noise of the original signal. Thus, our method can be considered as a suitable indicator of signal quality in frequency domain.

The weights are updated every 15 minutes to adapt to the change of the grid. The combining is performed at the highest

harmonics. Since low harmonics have a smaller range, we use spline interpolation to expand the frequency information for smaller harmonics. The weights are chosen as the signal power level to noise power level. Let f_{cmax} denote the frequency where the combined signal reaches its peak at the highest harmonics. The ENF of current segment is set as f_{cmax}/k_{max}, where k_{max} is the highest number for harmonics.

1) Error Correction Coding: For the sound signal, our proposed method could suffer from large noise power or interference in a short period. In this case, the estimation will demonstrate a case, where the ENF will jump up/down more than 0.1Hz and jump down/up within neighboring segments. This case is unlikely in reality. The reason is that, even ENF is dropped suddenly due to sudden large load or loss of generator, it takes at least $15s$ [4] for power generation factory to adjust generation to make up the loss. Motivated by above effects, we propose a simple yet efficient method to correct errors within neighboring segments.

The proposed error correction method utilizes the fact neighboring segments shouldn't demonstrate jump up/down and them jump down/up. Let $D(i)$ denote the ENF jump for ith segment, thus $D(i) = ENF(i+1) - ENF(i)$. The jump back and forth event is identified if all the following conditions are met:

- Jump has different direction, namely $D(i)D(i+1) < 0$;
- Jump value is larger than a threshold D_t, namely $|D(i)| > D_t$ and $|D(i+1)| > D_t$, where $|x|$ is the absolute value of x.

C. ENF Examples

In this subsection, we show the ENF signal we extracted from the training dataset using the algorithm we proposed.

1) With Power Signal : Fig. 3 shows the ENF signal from using power signal for grid A, C and I, whose nominal ENF is 60Hz. There are several characteristics we can see,

- All the three grids have small variation range;
- Grid A and C tend to go back to 60Hz more quick than grid I.

Fig. 4 shows the ENF signal from using power signal for grid B, D, E, F, G and I, whose nominal ENF is 60Hz. There are several characteristics we can see,

- Grid B is least stable among all the grids. Its mean deviates from nominal frequency significantly, and it has variation range up to 1.9Hz.
- Grid D, E are similar in terms of variation.
- Grid F seems to be the most stable one.
- Grid G and H have larger variation range than Grid D and E, but are stable than grid B. Grid G has variation up to 0.4Hz whereas Grid H has variation range up to 0.5Hz.

2) With Sound Signal: We show the ENF signal we extracted from the sound signal.

Fig. 5 shows the ENF signal from using power signal for grid A, C and I, whose nominal ENF is 60Hz. There are several characteristics we can see,

- Grid I has larger variation than Grid A and C, and goes back to 60Hz less frequently compared to Grid A and C;
- The differences shown in the three grids obtained from sound signal are similar to that obtained from power signal.

Above observation suggests that we could use the statistics obtained from power signal as ground truth for classification based on sound signal.

Fig. 6 shows the ENF signal from using sound signal for grid B, D, E, F, G and H, whose nominal ENF is 50Hz. There are several characteristics we can see,

- Grid B has the largest variation range and the largest deviation from nominal frequency;
- Grid D, E and F are more stable than other, and Grid F goes back to nominal frequency quicker than grid D and E;
- Grid H is less stable than grid G;
- All above trends are the same as what we observe from ENF obtained from power signal.

III. Location Classification

In this section, we utilize extract features in frequency domain and time domain, and then we adopt SVM for classification.

A. Features

The frequency features we adopted include, mean, variance, and range of the ENF signal, the ratio of the amplitude of first harmonic, denoted by f_1, to the third harmonics, denoted by f_3, as well as the wavelet decomposition for L level using 'db5' wavelet [5]. The left column of Table I lists all the features we have tested in this project in frequency domain.

TABLE I: Features Considered

Frequency Domain	Time Domain
Mean of ENF	Crest factor
Variance of ENF	Wavelet decomposition
Wavelet decomposition	
Range of ENF	
Ratio of f_1/f_3	

We also include the time domain information, including crest factor and wavelet decomposition. The crest factor is the ratio of the peak voltage to the root mean square (rms) of a current waveform. Let $C(i)$ denote the crest factor for the ith segment. For a perfect sinusoidal waveform, the crest factor $C(i)$ should be $\sqrt{2}$. Crest factor is an effective metric to evaluate the distortion of the sine waveform in grid [4], especially for the signal impacted by the misalignments between multiple harmonics. Consider two signals with the same first and third harmonics in amplitude. For one signal, the two harmonics are aligned, whereas for the other signal, the two harmonics have opposite phase. In this case, amplitude information of frequency cannot tell them apart, whereas crest factor can. The right column of Table I lists all the features we have tested in this project in time domain.

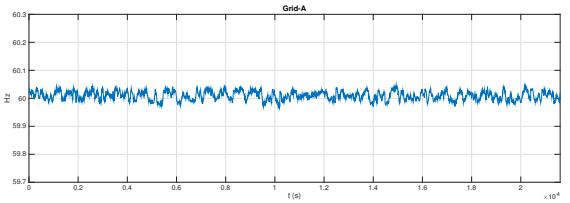

(a) Grid A

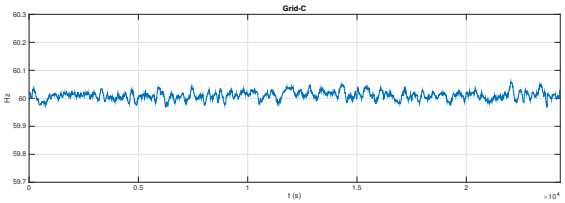

(b) Grid C

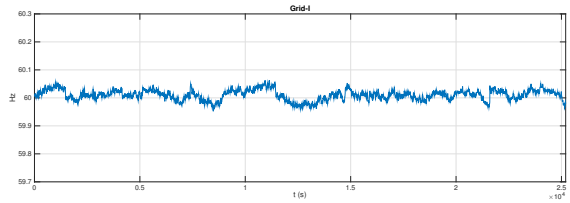

(c) Grid I

Fig. 3: ENF of Grid with Nominal Freq. 60Hz from Power Signal

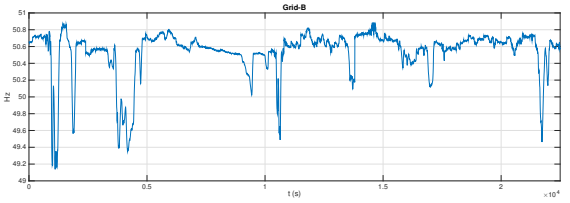

(a) Grid B

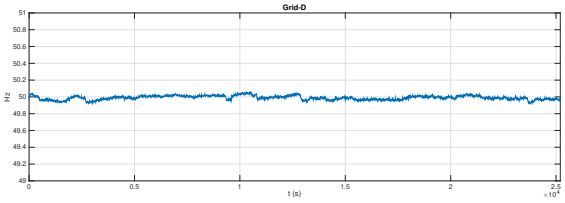

(b) Grid D

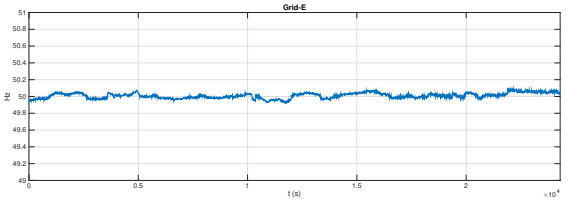

(c) Grid E

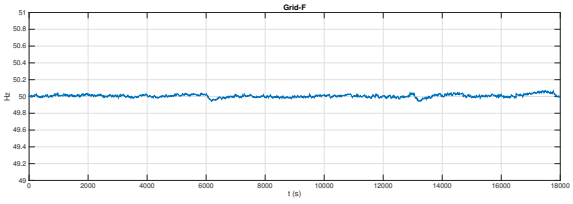

(d) Grid F

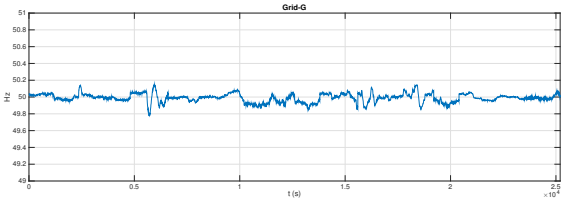

(e) Grid G

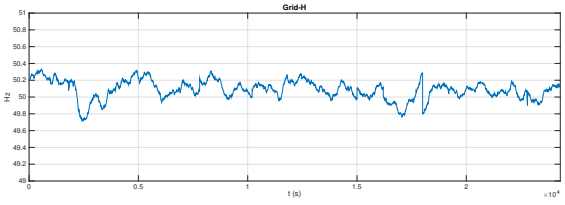

(f) Grid H

Fig. 4: ENF of Grid with Nominal Freq. 50Hz from Power Signal

B. Classification based on Nominal Frequency

To improve efficiency of classification, we first perform classification based on nominal frequency. Specifically, we compare the values of the maximum for PSD near 50Hz, 60Hz and their higher harmonics. If the value of maximum near 50Hz is larger than that near 60Hz, we consider the nominal frequency is 50Hz, and vice versa.

To address the issue that sound signal could be very noisy, and the estimation from a single segment could be wrong, we propose a voting scheme to improve the robustness of nominal frequency estimation. Specifically, we randomly select $N_s s$ segments in first few minutes, where $N_s s$ is chosen as an odd number. For each segment, we estimate its nominal frequency, vote for corresponding frequency. Whichever frequency gets the highest votes is regarded as the nominal frequency for current file.

C. Classification based on Source Type

As shown in [2], either to use power signal to classify sound file or to use sound signal to classify power signal, could result in low accuracy. This motivates us to separate signals based on their source type. It is observed that power

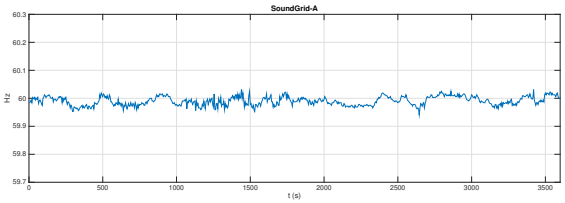

(a) Grid A

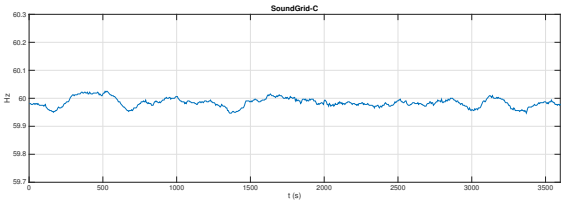

(b) Grid C

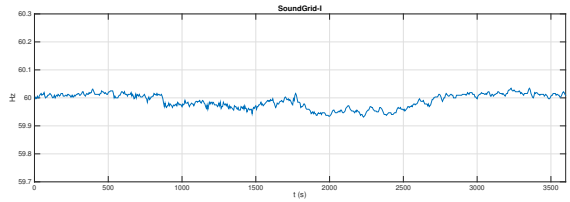

(c) Grid I

Fig. 5: ENF of Grid with Nominal Freq. 60Hz from sound Signal

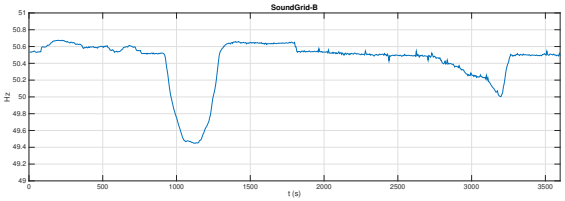

(a) Grid B

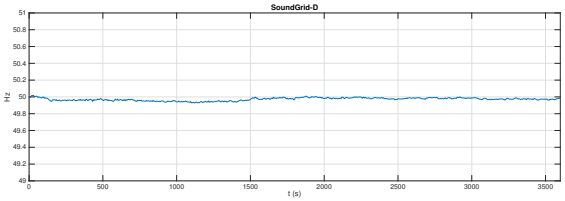

(b) Grid D

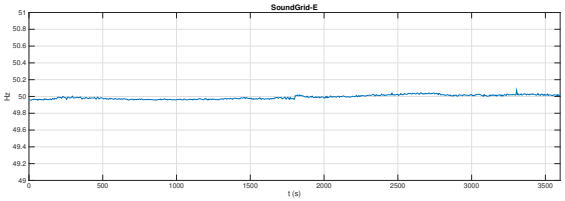

(c) Grid E

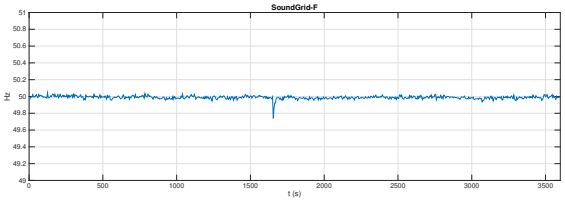

(d) Grid F

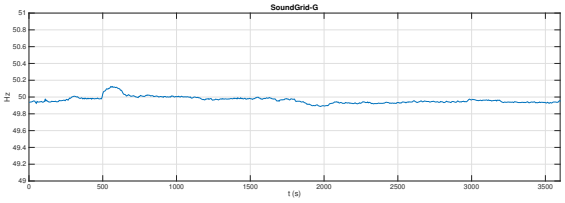

(e) Grid G

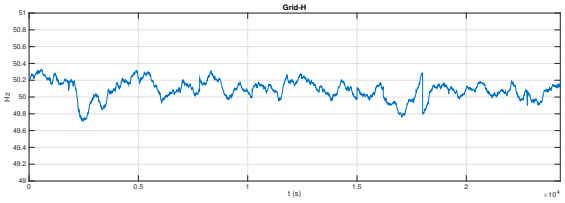

(f) Grid H

Fig. 6: ENF of Grid with Nominal Freq. 50Hz from sound Signal

signal has significant less noise than sound signal, especially for the spectrum between neighboring harmonics. Moreover, these noises tend to spread out the whole spectrum. Thus, we calculate average noise power for signal with 5 minutes duration, and use a threshold TH_{nf} to determine the file type. If the calculated average power level is larger than TH_{nf}, the file is considered to be a sound file. Otherwise, the file is considered as a power file.

D. SVM for Classification

We use LibSVM library as our SVM tools for classification [1]. Specifically, we use non-linear radial basis function kernel for multi-class classification. The parameters of the kernel, the cost parameter C and a parameter γ, are chosen via cross validation. Note that LibSVM utilizes a one-on-one classifier and a voting scheme for multi-class classification. Thus, our previous classification based on nominal frequency and source type could reduce the complexity of voting scheme. Weights are utilized to address the unbalanced training dataset problem [2].

E. None of Above Option

Whenever the classification result has low confidence, we compare the confidence rate to a threshold. If the confidence

rate is smaller than the threshold, we consider the grid tested does not belong to any training grid. Here, the sound file and power file have different thresholds. Since grid signals are cleaner, the classification are usually higher than that based on sound signals.

F. Feature Selection

We first use cross validation to evaluate the effectiveness of different features, and then we select the features with the highest accuracy rate for training and prediction. So far, we have four categories, which are classified based on nominal frequency and file type. As observed from previous chapter, different categories may have different features. For example, for the 50Hz group, both the ENF from sound and grid show that ENF range is a good criteria to tell Grid B from other Grids. As a result, the ENF range should be used as a feature. Yet for the 60Hz group sound file, the three grids have similar ENF range. Thus, ENF range would cause confusion for classifier to tell the three grids apart.

To evaluate the effectiveness of different features, we compare the accuracy for classification using individual feature and their combinations. Table II summarizes our findings. We use F_3 to represent frequency statistics, including mean, variance and range, F_w to represent the wavelet decomposition for ENF, F_r to represent the ratio of f_1/f_3, F_{all} to represent all frequency domain features, T_w to the wavelet decomposition information of the time domain signal, T_c to represent the crest factor.

As we can see from Table II, for Grid with 60 Hz, the maximal accuracy is achieved when the ratio of f_1/f_3, crest factor and wavelet decomposition in time domain are selected; for Grid with 50 Hz, the maximal accuracy is achieved when the statistics of ENF, the ratio of f_1/f_3, crest factor, wavelet decomposition in time domain are selected; for sound with 60 Hz, the maximal accuracy is achieved when only wavelet decomposition in time domain is selected; and for sound with 50Hz, the maximal accuracy is achieved when the crest factor and wavelet decomposition in the time domain are selected.

The results shown in Table II are expected. Take the Grid 50Hz and Grid 60Hz for example. We have explained based on observation, the statistic of ENF, such as range, offers limited information to classify grids operating at 60Hz, whereas for grids operating at 50Hz, ENF range could be useful. It is interesting to see that for sound signals, maximal accuracies are achieved when only time domain statistics are selected. Part of the reason is that the ENF signal extracted from the sound signal might be less accurate than the the ENF signal extracted from the grid signal.

G. Practice Dataset

We test the performance of our four categories based classification scheme with practice dataset. The accuracy of our estimation is 94%. The estimation on item 18, 21 and 47 is wrong. Both item 18 and 47 are supposed to 'None of above options', yet they are classified to grid C. The confidence level for item 18 and 47 estimation are 96% and 89%, respectively. This result suggests that the features selected for sound 60Hz are insufficient to differentiate grid C and another Grid in the practice dataset. The other error is item 21. It is a sound signal for a grid operating at 50Hz. Our estimation indicates grid F with confidence level of 58%. The ground truth is grid H. It is the second choice in our classification system with confidence level of 22.5%.

H. Test Dataset

Using our proposed classification scheme, the estimation of test dataset are performed.

I. Source Code Explanations

In this project, we submit the source code due to the usage of some executable files of libSVM. After unzipping the compressed file, the user needs to

Set Path Add the unzipped folder, including subfolders, to the Matlab path. Make sure that subfolder libsvm-3.21 is added. Users can right click the libsvm-3.21 folder, choose "Add to Path", and then choose "Selected Folders and Subfolders".

Call judgement.m Use function
$[Label, Conf] = judgement(Ori, Outloc, N)$.
For test purpose, Set
$Ori =' Testing\_dataset/Test\_'$;
$Outloc =' Testing\_result/'$;
$N = 100$;
$Label$ contains the estimated grid label and $Conf$ is a vector contains the confidence level for each estimation.

IV. Circuit Design and Data Analysis for ENF Acquisition

A. Hardware Design for the Sensing Circuit

In this section, we design a sophisticated sensing circuit for sampling real-time voltage signal out from power jack in our region. The circuit design is explained and justified component by component. The data acquisition was taken in household and university campus, with five hours of each location, at ten time slots, with each slot of one hour length. A preliminary analysis on acquitted data is conducted from theoretical point of view.

1) Transformer And Voltage Divider: A transformer is firstly introduced to our circuit in order to downgrade 110 AC to a safe range for both human beings and the sensing circuit without sacrificing the natural frequency features from power grid. Due to reality constraint, the maximum ratio, N1/N2, which we can acquire is 115/12.6 = 9.1, where n1 represents the number of turns at primary winding and n2 represents the number of turns at secondary winding. According to the equation V1/V2 = N1/N2 where V1 is primary voltage and V2 is secondary voltage, the secondary voltage is calculated as V2 = V1*N2/N1 which is 12.08V AC in our case. However, this voltage strength still exceeds 3.3V which is the limit of Analog-Digital-Converter (ADC) on Arduino Zero.

A simple but effective voltage divider is introduced right after we can source the downgraded AC voltage from transformer. Since the range of ADC is from 0 V to 3.3 V, we

TABLE II: Accuracy Test for Feature Selection

	Grid 60Hz	sound 60Hz	Grid 50Hz	sound 50Hz
F_3	57.333%	69.44%	61.46%	59.72%
F_w	78%	69.44%	64.93%	45.83%
F_r	98.67%	61.11%	88.54%	65.28%
F_{all}	88%	80.556%	92.71%	75%
F_3 + F_w	78%	72.22%	75.35%	55.56%
F_r + F_w	88%	83.33%	88.89%	66.67%
F_r + F_3	96.67%	72.22%	90.63%	83.33%
T_w	95.34%	**91.67**%	98.27%	97.22%
T_c	98%	69.44%	86.11%	47.22%
T_c + T_w	98%	86.11%	98.96%	**100**%
T_c + T_w +F_3	96%	75%	98.96%	94.44%
T_c + T_w +F_r	**98.67**%	86.11%	98.26%	98.61%
T_c + T_w +F_r + F_3	96.67%	88.89%	**98.96**%	94.44%
T_c + T_w +F_{all}	96%	80.55%	97.91%	88.88%

propose to have input signal ranging from 0.1 V to 3.2 V to neither burn the ADC pin nor be clipped. As a result, the downgraded voltage signal is 1.55 V AC. Therefore, the ratio of two resistor-blocks is 1.55/(12.08-1.55) = 0.15. Due to the limited variety of resistors package, we build the voltage divider by using R1 = 1$k\Omega$ and R2 = 220 Ω and R3 = 470 Ω whose ratio of R1:R2//R3 is calculated as 0.19 as expected.

2) Analog Digital Converter And Bias Voltage: For sampling real-time data, an Arduino Zero board is utilized because of three reasons. First of all, it provides us with a higher resolution of Analog Digital Converter, which can reach as high as 12 bits while other type of Arduino board such as Mega only allows 8 bits of resolution. Second, its clock owns a faster processing speed than any other Arduino board like Arduino Uno, where Arduino Zero owns a 48 MHz clock whereas Arduino Uno only owns a 16 MHz clock. The higher clock speed renders more stability while sensing signal at 1 kHz since it reduces actual time required for analog reading and data sending thus stabilizes data sampling at 1 kHz. Thirdly, in general Arduino board is easier to setup compared with other programmable board such as Raspberry Pi.

However, as an ADC pin, it does not take any value above 3.3 V or below 0 V. Thus, a DC biased voltage is needed to shift the transformed voltage up by 1.55 V so that sinusoid wave never goes below zero and above 3.3. Since Arduino Zero provides with a 3.3 V DC supply, we propose to source from there with a voltage divider involved. Such a voltage divider is expected to split 3.3 V to 1.63V and 1.67 V with which we can avoid negative signal input. Thus, we utilize a R4 = 100 $k\Omega$ and (R5 = 100+R6 = 2.2) $k\Omega$resistors to achieve so. The resultant sinusoid wave ranges from 0.25 mV to 3.25 V as expected and allowed.

3) External Clock: As the internal clock in Arduino Zero has a offset of 120 seconds per year, which is roughly 3 microseconds per second. Thus, an idea of an external clock comes in our mind to guarantee sampled data as frequent as 1024 Hz. The module named DS 3231 is introduced as an external clock source for Arduino Zero to clock data accurately. DS 3231 is setup in such a way that it sends 1024 square waves via its Square Wave (SQW) pin. In order to sample signal at such frequency, an interrupt is introduced in Arduino Zero so that it can sample data one time once a rising edge occurs. As a result, 1024 samples is sensed every second under this configuration. Furthermore, since the voltage coming out from SQW pin has a value of 4.85 V which exceeds the upper bounds of a digital pin on Arduino Zero, we lower down the voltage by paralleling a 10 $k\Omega$ resistor and a 2.2 $k\Omega$ resistor. This is simply because the SQW pin acts as a voltage node rather than a voltage source.

4) Possible Cause of Signal Noise: Severe Weather Condition A severe weather condition might cause significant fluctuation in the sampling data set. As known, power is transmitted through transmission line which exposes to outdoor environment. As one of our sampling data sets has shown, much more of noise occurred compared with other data sets when we sampled data at 18th Jan 2016 where a heavily snow swept over most of Ontario cities, including waterloo.

Capacitor Tank And Inductor Capacitor in household used equipment has a significant impact on the sampling data that we acquired from home where much more noise can be seen from sensing data. In addition, since our home-sensing data are from one of unit in an apartment building rather than a single house, electrical action produced from neighbors can also be an important factor that affect real-time signal. This can also be demonstrated as in Fig. 8.

B. Data Analysis

In the part, we first show the ENF info of our recording and discuss which grid is shared most similarity with in the training dataset.

1) ENF Info.: The ENF info of our recording signal is shown in Fig. 9. The Fig. 9(b) and the Fig. 9(c) show the ENF for recordings at home and at university, respectively. As we can see, the nominal frequency of the waterloo grid is 60Hz, which is the same as grid A, C and I in the training dataset. The variation of ENF for the waterloo grid looks small, with range less than 0.1Hz, and the variation of ENF looks smaller than the variation at home.

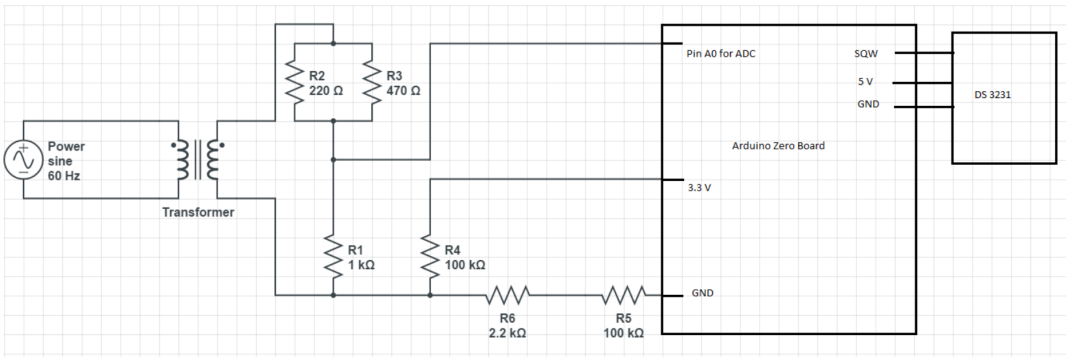

Fig. 7: Schematic

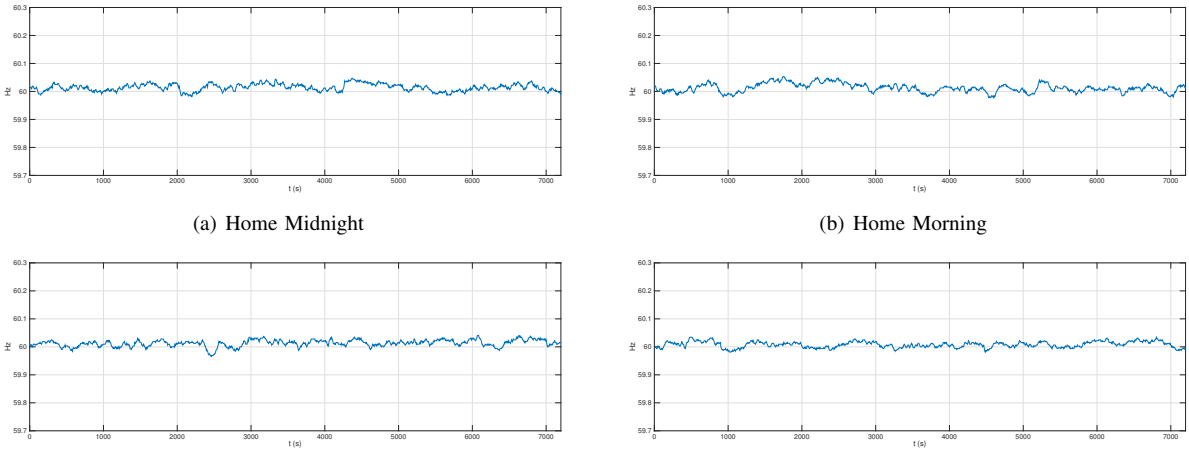

(a) Home Midnight

(b) Home Morning

(c) University Morning

(d) University Afternoon

Fig. 9: ENF Info for Grid at Waterloo, Ontario

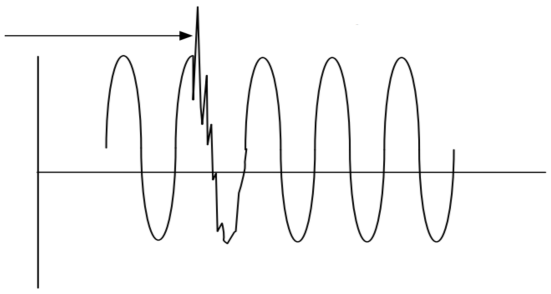

Fig. 8: Distorted Signal

2) Waterloo Grid is part of Grid C: We use the proposed classifier to determine the waterloo grid belongs to which grid in the training dataset. We clip 10 minutes long signal from each recording, and estimate their grid respectively. For 4 test files, our classifier outputs all indicate waterloo grid is part of grid C with the same confidence level of 47.6%. Since the confidence level is low, we consider waterloo grid belongs to "None of Above Options".

V. Conclusion

In this project, we have proposed to utilize features in both time domain and frequency domain to improve classification accuracy. Specifically, we propose to utilize crest factor in time domain and the ratio of f_1/f_3 in frequency domain as indicators of the distortion of power signal. Moreover, we have proposed to categorize signals based on the nominal frequency and source type to improve efficiency of the classifier. Through cross validation, we identify the most effective features for different categories to further enhance accuracy. On the practice

dataset, our proposed algorithm can achieve accurate rate of 94%. We have also designed and built a circuit with accurate timing for power signal acquisition.

REFERENCES

[1] Chang, Chih-Chung and Lin, Chih-Jen, "LIBSVM: A library for support vector machines," *ACM Transactions on Intelligent Systems and Technology (TIST)*, vol. 2, no. 3, pp. 27, 2011.

[2] Hajj-Ahmad, Adi and Garg, Ravi and Wu, Min, "ENF-Based Region-of-Recording Identification for Media Signals," *Information Forensics and Security, IEEE Transactions on*, vol. 10, no. 6, pp. 11251136, 2015.

[3] Oppenheim, Alan V and Schafer, Ronald W and Buck, John R and others, "Discrete-time signal processing" *Prentice-hall Englewood Cliffs*, vol. 2, 1989.

[4] Bollen, Math H and Gu, Irene, "Signal processing of power quality disturbances' *John Wiley & Sons*, vol. 30, 2006.

[5] Mallat, Stephane, "A wavelet tour of signal processing: the sparse way" *Academic press*, 2008.

Qinghua Shen [IEEE S'11] is currently working as a postdoctoral fellow at the Broadband Communications Research (BBCR) Group, University of Waterloo, Canada. He obtains his Ph.D. degree at the department of Electrical and Computer Engineering of the University of Waterloo in 2015, and the master and the bachelor degrees in Electrical Engineering from Harbin Institute of Technology in 2010 and 2008, respectively. His research interests include resource allocation and signal processing for e-healthcare system.

Wei Zhang [IEEE S'12] is currently a fourth year student at the electrical and computer engineering department of University of Waterloo, Canada. He previously worked as an intern for multiple organizations, among them are Microsoft Research Asia and Vodafone. His research interests include image processing and machine learning.

Edrick Wong [IEEE S'14] is currently a second year student at the system design engineering department of University of Waterloo, Canada. He previously worked as an Hardware intern for Apple Inc. in California.

Brady Kieffer [IEEE S'14] is currently a second year student at the system design engineering department of University of Waterloo, Canada. He previously worked as an trading associate intern for TD Canada Trust, and data scientist intern for Capital One.

Xuemin (Sherman) Shen [IEEE M97-SM02-F09] received the B.Sc. degree from Dalian Maritime University, Dalian, China, in 1982, and the M.Sc. and Ph.D. degrees from Rutgers University, New Brunswick, NJ, USA, in 1987 and 1990, respectively, all in electrical engineering. He is a Professor and University Research Chair with the Department of Electrical and Computer Engineering, University of Waterloo, Waterloo, ON, Canada. His research focuses on resource management in interconnected wireless/wired networks, wireless network security, wireless body area networks, smart grid, and vehicular ad hoc and sensor networks.
Dr. Shen is a registered Professional Engineer of Ontario, Canada, a Fellow of the Canadian Academy of Engineering, a Fellow of the Engineering Institute of Canada, and a Distinguished Lecturer of the IEEE Vehicular Technology Society and IEEE Communications Society.